JST: Engineering and Technology for Sustainable Development
Volume 33, Issue 4, October 2023, 041-048

Research for the Production of Environmentally Friendly Material from Industrial Waste Stone Powder by Geopolymer Technology

Pham Anh Tuan [1,2], Nguyen Thanh Cong[2], Bui Chuong[3], Ha Thu Huong[2*]
[1]Faculty of Biotechnology, Chemistry, and Environmental Engineering, Phenikaa University, Ha Noi, Vietnam
[2]Polymer R&D Center, A&A Green Phoenix Group JSC, Ha Noi, Vietnam
[3]School of Chemical Engineering, Hanoi University of Science and Technology, Ha Noi, Vietnam
[*]Corresponding author email: huong.hathu@phenikaa-uni.edu.vn

Abstract

Geopolymer technology was applied for environment friendly material fabrication with 20 - 23 wt% waste stone powder from artificial stone production process and 0.5 wt% of Na_2SiO_3 liquid glass (39 wt%). The material met the technical requirements according to TCVN 6477:2016 standard for unburnt material. The time of co-hydrolysis reaction help to create the Si-O-Si interspersed with bonds was not affected by the curing process of PCB40 with the presence of liquid glass ($Na_2SiO_3.nH_2O$). We are creating a geopolymer network and helping the material reduce brittleness and increase ductility and compressive strength of conventional cement. The peak region at 959 cm^{-1} of FT-IR analysis and the surface structure morphology of SEM images showed that the Si-O-Al/Si-O-Si bond was formed by the reaction of Na_2SiO_3 with cement. The surface of the geopolymer material is denser and more tightly bound than the sample without Na_2SiO_3. The manufacture of unburnt materials from waste stone powder from the artificial stone production process by TCVN 6477:2016 can open a new treatment direction for this type of waste, reducing the harmful effects of landfill on the environment.

Keywords: Geopolymer, sodium silicate, unburnt materials, waste stone powder.

1. Introduction

Geopolymer technology was first introduced by Joseph Davidovits in 1978 and developed rapidly. Many materials are studied to create geopolymers and applied in many fields [1]. Geopolymer has been studied based on fly ash (FA) and blast furnace slag (GGBS) as a mortar to patch concrete cracks with water repellence, hydrophobicity, fast curing, and high strength. Zailaini *et al.* [2] successfully studied an FA-based geopolymer adhesive with compressive strength and adhesion strength of 95 MPa and 11 MPa, which is sufficient for coated concrete (OPC). Rosyide *et al.* [3] studied the effect of geopolymer on asphalt when adding 5% geopolymer improved the structural chain mobility and storage stability of asphalt. Geopolymer is also studied in 3D printing; with 50% GGBS and 50% FA, geopolymer concrete has good enough compressive strength for construction works [4]. By-products from industrial production or mining are often used to produce geopolymers. Flying ash with high free CaO content is widely used and creates many outstanding advantages [5]. GGBS, as a by-product of the iron-smelting process, has also been chosen by many research groups. GGBS to partially replace cement in the geopolymer, resulting in less exothermic hydration and reducing the risk of cracking. Recently, red mud (RM) has also been used in geopolymer technology, thanks to the alkalinity available in RM, which reduces the cost of geopolymer production. RM can also replace FA, changing the required amount of NaOH and curing conditions, but geopolymer is likely to give higher strength [6]. Geopolymer material consisting of Rice husk ash (RHA) with nano-SiO_2-rich composition has helped to reduce pollution problems caused by landfill, especially in rice-producing countries and self-inserting material as well produced from RHA by geopolymer technology [7]. In Vietnam, there have been many studies on geopolymer materials and the use of wastes from industrial production or mineral extraction [8]. However, there is no research on the waste stone powder from the production process. This successful research will open a new treatment direction for waste stone powder, which can be reused to make unburnt, environmentally friendly materials, reducing the impact on the environment caused by the material. Landfill causes and is consistent with the development trend of unburnt materials today.

2. Materials and Methods

2.1. Materials

Waste stone powder used for research is obtained from artificial stone manufacturers belonging to Phenikaa Group, Vietnam, whose main ingredient is SiO_2. $Na_2SiO_3.nH_2O$ solution from Viet Tri Chemical Joint Stock Company has a Na_2SiO_3 content of 39 wt%

ISSN 2734-9381
https://doi.org/10.51316/jst.169.etsd.2023.33.4.6
Received: April 18, 2023; accepted: August 9, 2023

and sodium silicate module of 2.68 with moderate viscosity of 60 mPas. PCB40 Portland cement from Vissai Ninh Binh, Vietnam, has a compressive strength (after 28 days) of 43 ± 1 MPa, fineness grain size 0.09 mm of 0.8 ± 0.1%. The specific surface of 4200 ± 100 cm^2/g (according to the Blaine method), and SO_3^{2-} content of 2.0 ± 0.1. Chemical compositions of PCB40 Vissai Ninh Binh is shown in Table 1. Aggregation crushed stone ≤ 5 mm with the main component SiO_2 (~84 wt%) is quarried in Hoa Binh, Vietnam. Clean water originates from the Hanoi water factory with no impurities such as heavy metals or organic impurities.

2.2. Methods

The setting time of cement is determined according to TCVN 6017:2015 standard at the Institute of Building Materials, Ministry of Construction. Fourier transform infrared (FT-IR) spectra were measured on Spectrum Two Perkin Elmer instrument, USA. Thermogravimetric analysis (TGA) was measured on a TGA 4000 instrument, Perkin Elmer, the USA, under the unisothermal mode; the temperature increased from 25 ºC to 900 ºC at a rate of 10 ºC/min, airflow 2.5 litters/hours. Scanning electron microscopy (SEM) images were observed by the instrument S-4800, Hitachi, Japan. The compressive strength was measured on the AD 200/EL instrument, Unit Test, Malaysia. The particle size of waste rock powder was measured on LA-960, Horiba, Japan.

3. Results and Discussions

3.1. Characteristics of the Industrial Waste Stone Powder Composition

Waste stone powder from the production of artificial stone at factories were brought to the settling and dry pressing systems according to the plate filter technology; the moisture content of the powder after pressing is about 30 ÷ 33 wt%. The waste stone powders after drying at 110 °C for 24h were sampled, tested, and analysed; the results are presented in Table 2.

The analysis results from Table 2 show that the waste stone powder from the production process is relatively stable in terms of particle size and chemical composition, which allows the assumption that the waste stone powder composition is stable and constant during the research and testing in the following sections.

Table 1. Chemical compositions of PCB40 Vissai Ninh Binh

Oxides (wt%)	CaO	SiO_2	Al_2O_3	SO_3	Fe_2O_3	K_2O	Na_2O	MgO
PCB40 The Vissai	63.72	21.91	6.85	0.41	4.14	0.63	0.28	2.06

Table 2. Characteristics of waste stone powder from the artificial stone factory

No	Characteristics	Unit	M1	M2	M3	M4	M5	M6	M7	M8	M9	M10
1	SiO_2 ratio	%	83.72	82.91	83.57	83.69	83.87	83.94	83.92	83.88	83.79	83.91
2	Organic impurities (*)	%	13.90	13.82	13.96	13.87	13.86	13.94	13.91	13.86	13.85	13.95
3	Inorganic impurities (**)	%	2.38	2.28	2.39	2.36	2.39	2.37	2.34	2.38	2.39	2.37
4	Size of particles											
	< 10 µm	%	23.98	26.14	25.84	22.91	24.35	21.78	22.65	23.81	23.49	25.07
	< 20 µm	%	56.44	58.63	59.18	54.67	55.82	57.39	54.46	56.24	57.21	53.72
	< 30 µm	%	74.18	75.21	76.34	72.86	73.42	74.94	75.12	73.68	71.84	74.57
	< 45 µm	%	86.58	87.42	86.78	85.97	87.24	86.38	87.12	85.69	86.81	87.23
	> 45 µm	%	13.42	12.98	13.22	14.53	12.76	13.62	12.88	14.31	13.19	12.77

(*) Cured unsaturated polyester resin in artificial stone.
(**) Other additives in artificial stone such as inorganic pigments.

3.2. Study on the Formation of PCB-Na_2SiO_3. Bonding System

To investigate the bond formation between cement and Na_2SiO_3 solution to create a geopolymer network, we mixed $Na_2SiO_3.nH_2O$ with cement and determined the characteristics of the curing process according to the ratios of $Na_2SiO_3.nH_2O$ as 0; 2.5; 5 and 7.5%, respectively. The results of the cement setting process are presented in Table 3. The ratio of cement: water is determined at 4:1 according to the TCVN 6017:2015 standard.

Table 3. Setting time of material samples

No		M0	M1	M2	M3
1	Cement ratio: $Na_2SiO_3.nH_2O$	100 : 0	97.5 : 2.5	95 : 5	92.5 : 7.5
2	Cement: H_2O ratio	4 : 1	4 : 1	4 : 1	4 : 1
3	Setting starting time (min)	145	100	75	60
4	Setting ending time (min)	215	190	170	140

*The setting starting time and setting ending time were test according to the TCVN 6017:2015 standard

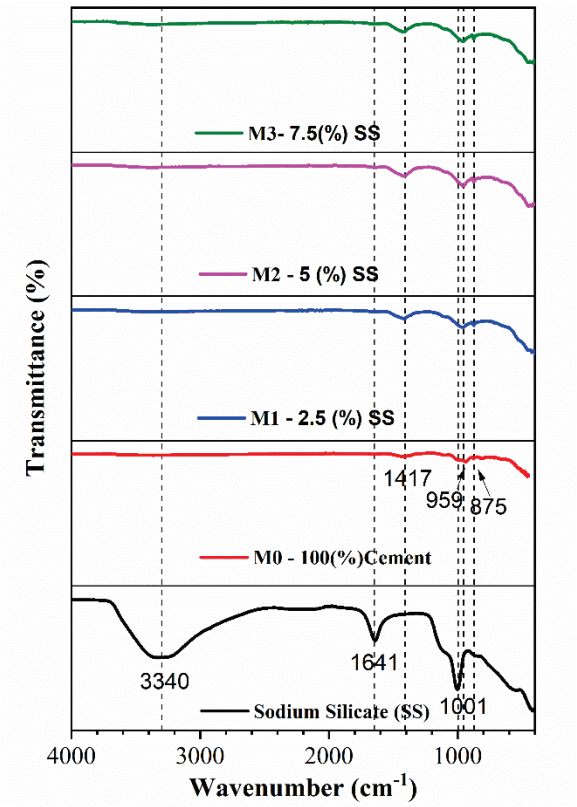

Fig. 1. FT-IR spectra of $Na_2SiO_3.nH_2O$ and M0, M1, M2, M3 after 28 days

The typical parameters for the setting process of cement are the starting time and the ending time. From the results in Table 3, $Na_2SiO_3.nH_2O$ promotes the setting time of cement. Specifically, the cement sample's starting time - ending setting increased from 145 min to 215 min, decreased from 100 min to 190 min in sample M1; from 75 min to 170 min in sample M2 and from 60 min to 140 min in sample M3. A too- fast setting time can cause stress, leading to cracking. Therefore, we only test $Na_2SiO_3.nH_2O$ content up to 7.5%. To determine if $Na_2SiO_3.nH_2O$ is involved in the cementation process, the FT-IR spectrum of $Na_2SiO_3.nH_2O$ and the samples above were analysezed from the fragment of sample compression after 28 days. FT-IR measurement results are presented in Fig. 1.

The results of FT-IR spectroscopy in Fig. 1 show that $Na_2SiO_3.nH_2O$ appears in the H-O-H bending vibrations (strain vibrations) and -OH stretching vibrations (valence vibrations) of the water molecules, which are observed between 1641 cm^{-1} and 3340 cm^{-1}, Si-O asymmetric bonds were observed between 1000 cm^{-1} [8]. While in the M0, M1, M2 and M3 sample, a peak of 1417 cm^{-1} appeared as a product of the carbonate process (C-O bond in $CaCO_3$); 959 cm^{-1} and 875 cm^{-1} characterize the bonds of Si-O and Al-O of cement [9]. The O-Al/Si-O-Si bond is also shown at 959 cm^{-1}, which is the peak occurring in geopolymer samples [10]. Thus, $Na_2SiO_3.nH_2O$ has removed the -OH group to form a spatial network interwoven with the network of regular set cement. The following reaction can explain this process:

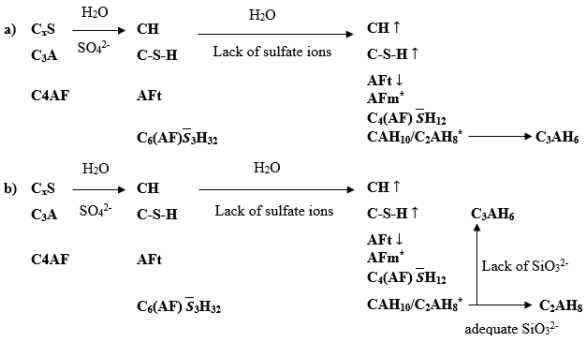

Fig. 2: Hydration of PCB40 cement and PCB40 cement in the presence of $Na_2SiO_3.nH_2O$

In this formular: C_xS, C_3A, C_4AF are calcium silicate (C_2S, C_3S), calcium aluminate, and calcium aluminoferrite minerals;

CH: $Ca(OH)_2$; C-S-H: $CaO.SiO_2.H_2O$; AFt: $C_6A\overline{S}_3H_{32}$: $3CaO.Al_2O_3.3CaSO_4.32H_2O$; AFm: $C_4A\overline{S}_3H_{12}$: $3CaO.Al_2O_3.CaSO_4.12H_2O$; C_3AH_6: $3CaO.Al_2O_3.6H_2O$; $C_6(AF)\,\overline{S}_3H_{32}$: $3CaO.Al_2O_3.\ Fe_2O_3.3CaSO_4.32H_2O$; $C_4(AF)\,\overline{S}H_{12}$: $3CaO.Al_2O_3.\ Fe_2O_3.CaSO_4.12H_2O$; C_2ASH_8: $2CaO.Al_2O_3.SiO_3.8H_2O$.

Symbols in Fig. 2 of ↑ and ↓ represent mass increase and decrease, and * represents new hydrates. PCB40 cement contains 5 wt% fly ash mineral additive compared to PC40 cement, in which, fly ash has the role of increasing plasticity and reducing the water ratio used in the mix. According to the diagram in Fig. 2a, in the absence of $Na_2SiO_3.nH_2O$, the cement hydration occurs similarly to ordinary PCB cement, and the obtained products include: CH, C-S-H, AFt, AFm, $C_4(AF)\overline{S}H_{12}$ and CAH_{10}/ C_2AH_8 and finally creating of C_3AH_6. The hydration reaction occurs in the presence of $Na_2SiO_3.nH_2O$, according to the diagram in Fig. 2b, CAH_{10}/ C_2AH_8 reacts with SiO_3^{2-} to form the mineral C_2ASH. C/Na - Al - Si - H bonds are formed, called geopolymer [11]. Thus, when the amount of Na2SiO3.nH2O is large enough, a geopolymer network is formed, and the curing speed of PCB40 cement also increases. When 2.5%, 5%, and 7.5% $Na_2SiO_3.nH_2O$ were used, the setting starting time of the system was reduced from 145 minutes to 100 minutes, 75 minutes, and 60 minutes, respectively; at the same time, the setting ending time was also reduced from 215 minutes to 190, 170 and 140 minutes, respectively. This can be explained because $Na_2SiO_3.nH_2O$ creates an alkaline environment, promoting the hydration of PCB cement. However, in the production of unburnt bricks, this difference is acceptable.

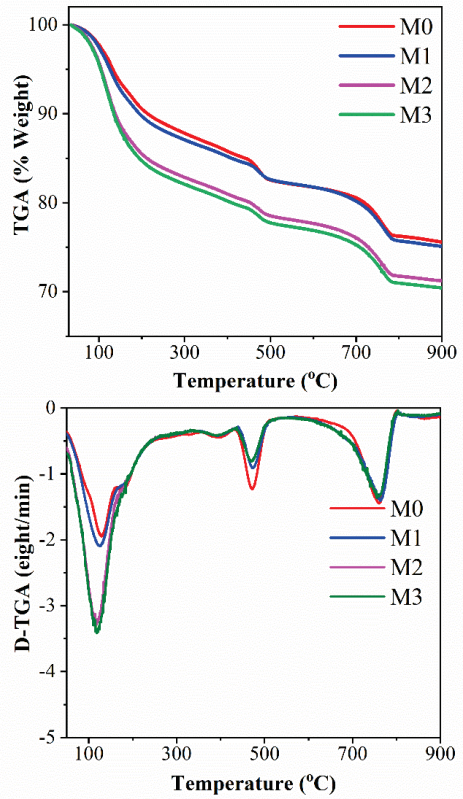

Fig. 3. TGA-DTGA diagram of $Na_2SiO_3.nH_2O$ and M0, M1, M2, M3 samples after 28 days

To determine the mass change of the cement-water binder system in the presence and absence of $Na_2SiO_3.nH_2O$, Thermal calorimetry analysis (TGA) of the samples M0, M1, M2, and M3 above was carried out after 28 days. The samples to test TGA were prepared from a fragment of the sample after the compression test and were finely ground to a particle size of less than 20 microns prior to analysis. The obtained results are shown in Fig. 3.

According to Fig. 3, with increasing of $Na_2SiO_3.nH_2O$, the mass loss (mass of water released) increased from M0 to M3 sample. At 100 °C, the mass loss of sample M0 is the least; sample M3 is the largest. The explanation is that when adding $Na_2SiO_3.nH_2O$ to the system, the -OH group of $Na_2SiO_3.nH_2O$ is separated, creating excess water. When raising the temperature to 100 °C, this amount of water evaporates, causing the sample's mass loss. At the same time, at this temperature, the formation of C-S-H, Ettringite bonds ($Ca_6Al_2(SiO_4)_3(OH)_{12}$-$26H_2O$), geopolymer C/Na-Al-Si-H is characterized by a peak in the DTGA curve [12].

At 490 °C, Ca $(OH)_2$ decomposes to form CaO and H_2O, with the maximum mass loss is obtained in the M3 sample. Rising the temperature to 780 °C, $CaCO_3$ decomposes into CaO and CO_2. However, at the temperature, the mass loss of all samples is insignificant because the amount of $CaCO_3$ were created from the sample with and without $Na_2SiO_3.nH_2O$ is similar. This is provided from the result of thermal decomposition of samples with and without Na_2SiO_3 in the Fig. 3 and also consistent with the results of the FT-IR spectrum in the Fig. 1.

To verify these statements, we measured the compressive strength of material samples from M0 to M3 according to the TCVN 6016:2011 standard. The obtained results are presented in Table 4.

Table 4. Compressive strength of the samples.

No	Compressive strength	Unit	TCVN 2682:2009	M0	M1	M2	M3
1	3 days	MPa	≥ 21	21	22	23	24
2	14 days	MPa	-	32	38	40	41
3	28 days	MPa	≥ 40	43	50	53	54

* Uncertainty of measurement: 0.59 Mpa

Table 4 shows the compressive strength of the samples after three days; when the geopolymer network started to form, the compressive strength increased from 21 ± 0.59 MPa gradually to 24 ± 0.59 MPa. However, the compressive strength increased from 43 ± 0.59 MPa gradually to 54 ± 0.59 MPa from sample M0 to sample M3 respectively after 28 days, which proves that when the material has formed a geopolymer network and stabilized, it has increased the plasticity of the material, i.e., increased compressive strength.

3.3. Investigate the Effects of Waste Stone Powder

Samples of the material were made with the main ingredients being stone powder and the cementitious system - $Na_2SiO_3.nH_2O$ to fabricate unburnt materials by geopolymer technology using waste stone powder as raw materials. Consider waste stone powder to replace sand according to the ratio of cement:sand:water in the TCVN 6016:2011 standard. Samples are fabricated according to the composition shown in Table 5. The material samples were analysed by FT-IR after 28 days and the results are presented in Fig. 4.

Table 5. Mixture of material samples.

Components	Unit	G0	G1	G2	G3
Cement PCB40	wt%	22	22	22	22
$Na_2SiO_3.nH_2O$	wt%	0	0.55	1.10	1.65
Waste stone powder	wt%	67	67.00	67.00	67.00
H_2O	wt%	11	10.45	9.90	9.35
Total	wt%	100	100	100	100
Cement ratio: $Na_2SiO_3.nH_2O$		100 :0	97.5 2.5	95:5	92.5:7 .5

* The samples M0, M1, M2, M3 were set according to TCVN 6016:2011 and measured after 28 days.

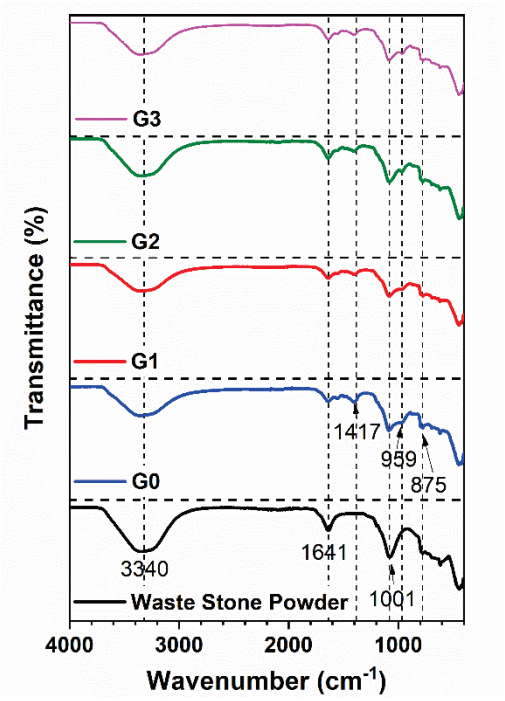

Fig. 4. FT-IR spectra of Waste Stone Powder, samples G0, G1, G2 and G3 after 28 days

The Fig. 4 shows that, the FT-IR spectra of samples waste stone powder, G0, G1, G2 and G3 appear characteristic peaks at 3340 cm^{-1}; 1641 cm^{-1}; and 1001 cm^{-1}, respectively, demonstrating the presence of the O-H and Si-O bonds. Besides, in sample G0, a peak of 1417 cm^{-1} of C-O bonds and 959 cm^{-1} of Si-O-Si bonds appeared similar to samples G1, G2, and G3, which can be explained by the fact that these samples have the same hydrolysis. This phenomenon shows that the cement and the admixture have been hydrated and exist in parallel with each other, in association with each other and the waste stone powder. It is further demonstrated when conducting morphological analysis of the structure of samples G0 and G2 (representative of samples with $Na_2SiO_3.nH_2O$) by SEM image in Fig. 5.

The compressive strength of samples G0, G1, G2, and G3 were measured to evaluate the influence of $Na_2SiO_3.nH_2O$ content on the material in the presence of waste stone powder according to the TCVN 6016:2011 standard. The results are presented in Table 6.

From Table 6, when $Na_2SiO_3.nH_2O$ is present, the material's compressive strength increases significantly. After 14 days, the compressive strength increased from 2.06 ± 0.59 MPa (G0) to 3.17 ± 0.59 MPa (G3). When the sample reached 28 days, the compressive strength of sample G0 was 3.95 ± 0.59 MPa, while samples G1, G2, and G3, respectively, reached 4.79; 5.72 and 6.08 (± 0.59 MPa). This result shows that the bond in the sample with $Na_2SiO_3.nH_2O$ is improved, and the ductility is higher, so the compressive capacity of the material is also higher than that of the sample without $Na_2SiO_3.nH_2O$, which is also consistent with the analysis results above.

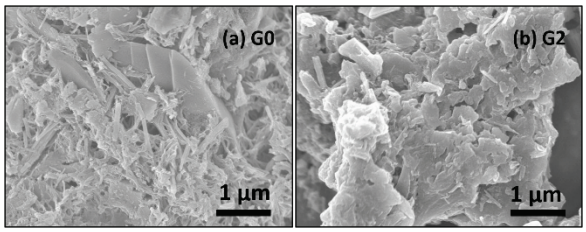

Fig. 5. SEM images of the fracture surface of samples (a) G0 and (b) G2

Table 6. Compressive strength of the samples

Compressive strength	Unit	G0	G1	G2	G3
14 days	MPa	2.06	2.34	2.68	3.17
28 days	MPa	3.95	4.79	5.72	6.08

* Uncertainty of measurement: 0.59 MPa

3.4. Fabrication of Unburnt Materials from Waste Stone Powder by Geopolymer Technology

Normally, the binder content in unburnt bricks is about 8-12 wt%. From the survey results of the cement binder system - $Na_2SiO_3.nH_2O$ and when there is waste stone powder above, a mixture has been characterized based on the TCVN 6477:2016 standard as a basis for studying and evaluating, we chose the binder content in unburnt bricks is 10 wt%. The composition of the unburnt materials is presented in Table 7 below:

Table 7. Compound formula of unburnt bricks

No	Component	Unit	Samples			
			C0	C1	C2	C3
1	Cement PCB40	wt%	10	10	10	10
2	$Na_2SiO_3.nH_2O$	wt%	0	0.25	0.5	0.75
3	Waste stone powder	wt%	20	20	20	20
4	Crushed stone	wt%	55	55	55	55
5	H_2O	wt%	15.0	14.75	14.5	14.25
	Total	wt%	100	100	100	100

Table 8. The compressive strength of unburnt bricks

No	TCVN 6477:2016	Unit	C0	C1	C2	C3
7 days	-	MPa	5.7	7.1	8.7	10.3
14 days	-	MPa	7.0	8.2	10.2	13.7
28 days	≥ 10	MPa	8.1	9.6	11.7	15.0

* Uncertainty of measurement: 0.59 MPa

From Table 7 and Table 8 show that, when using 20 wt% of waste rock powder in the composition of unburnt materials, samples using only cement (C0) and samples with 0.25 wt% $Na_2SiO_3.nH_2O$ (C1), the compressive strength did not meet the TCVN 6477:2016 standard. When increasing $Na_2SiO_3.nH_2O$ to 0.5 wt% (C2 sample) and 0.75 wt% (C3), the compressive strength after 28 days exceeds the required value according to the TCVN 6477:2016 standard. On the other hand, according to the TCVN 8826:2011 standard, the additive content does not exceed 5 wt% of that of cement. Therefore, sample C2 is selected for further research.

3.5. The Influence of Waste Stone Powder Content

To select the optimal ratio of stone powder in the fabrication of unburnt materials, formula C2 with a constant cement content of 10 wt% and fixed $Na_2SiO_3.nH_2O$ was used, and the amount of crushed stone and waste stone powder was changed according to the below samples.

Table 9. Proportion alteration of waste stone powder in the mixture

No	Component	Unit	Samples			
			F0 (C2)	F1	F2	F3
1	Cement PCB40	wt%	10	10	10	10
2	$Na_2SiO_3.nH_2O$	wt%	0.5	0.5	0.5	0.5
3	Waste stone powder	wt%	20	23	26	29
4	Crushed stone	wt%	55	52	49	46
5	H_2O	wt%	14.5	14.5	14.5	14.5
	Total	wt%	100	100	100	100

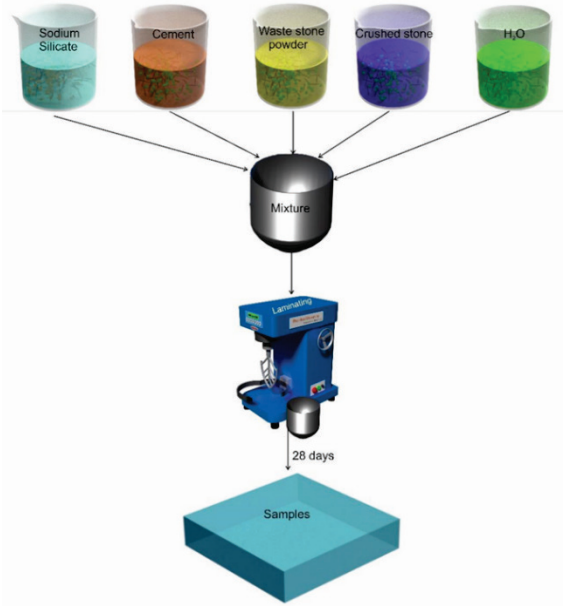

Fig. 6. Production process of unburnt bricks by geopolymer technology.

The fabrication processing of unburnt material samples is carried out according to the diagram in Fig. 6, and the images of obtained samples were shown in the Fig. 7. After fabrication, the unburnt material sample was cured in a sheltered house and measured according to TCVN 6477:2016 standard. The results are presented in Table 9.

Table 9 shows that, the samples have adequate water absorption and permeability when increasing the waste stone powder content in the mixture, according to the TCVN 6477:2016 standard. However, the compressive strength decreases gradually. The compressive strength of the F0 sample is 12.2 ± 0.59 MPa, and the value is reduced to 10.9 ± 0.59 MPa with the waste stone powder content of 23 wt% (F1 sample). Continuing to increase the

waste stone powder to 26 wt% and 29 wt% for samples F2 and F3, compressive strength decreased to 9.8 ± 0.59 MPa and 9.2 ± 0.59 MPa, respectively. According to the TCVN 6477:2016 standard, these samples do not meet the technical requirements. When the stone powder ratio increases, the compressive strength decreases. This result can be explained by the following reason: with a large amount stone powder with very fine particles in the formula, the amount of Na_2SiO_3 in the initial mix is not enough to participate in the co-hydrolysis reaction to create a geopolymer network linking all of the aggregate particles. This makes the material structure less stable, leading to a decrease in compressive strength. Thus, the F1 formula is more suitable for fabricating unburnt materials with geopolymer technology.

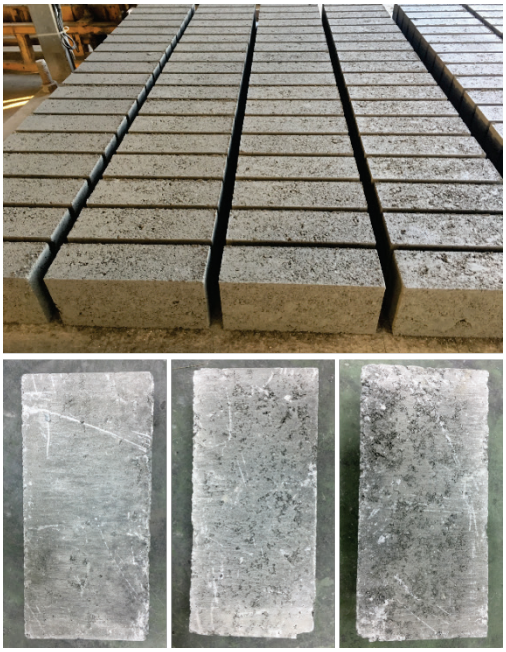

Fig. 7. Images of unburnt bricks from waste stone powder

Table 10. The technical parameters of unburnt bricks samples

No	Component	Unit	TCVN 6477: 2016	Samples F0 (G2)	F1	F2	F3
1	Compressive strength						
	7 days	MPa	-	9.5	8.8	7.7	7.3
	14 days	MPa	-	11	9.7	8.9	8.4
	28 days	MPa	≥ 10	12.2	10.9	9.8	9.2
2	Water absorption	%	< 12	7.5	8.3	8.9	9.5
3	Water permeability	l/m^2.h	≤ 16	12.2	12.4	12.5	12.7

* Uncertainty of measurement: 0.59 MPa

4. Conclusion

The addition of Na_2SiO_3 solution to cement created a cementitious binder system - Na_2SiO_3, in which the polymer space network formed by the polymerization reaction of liquid glass was interwoven with the cement crystal lattice. This can be seen in the FTIR analysis results in Fig. 4 and the SEM structure morphology in Fig. 5. When increasing the content of $Na_2SiO_3.nH_2O$, the hydration rate of cement also increases as shown in Table 3.

The compressive strength of the cement-$Na_2SiO_3.nH_2O$ system is significantly increased (up to 20-30%) in comparison with the cementitious system without $Na_2SiO_3.nH_2O$ when using waste stone powder.

FT-IR spectrum analysis shows that the waste rock powder is chemically bonded with the cement-solution Na_2SiO_3, and the SEM images show that the bonds between them are not simply stacked cross-links like ordinary PCB cement, created a solid structure and reducing the brittleness of the obtained unburnt brick. Besides that, the ductility of unburnt brick increased, as shown by the increase in compressive strength of the material from 3.95 ± 0.59 MPa in the sample without Na_2SiO_3 to 6.08 ± 0.59 MPa in the sample with Na_2SiO_3 after 28 days.

The Na_2SiO_3 solution helps improve the compressive strength and, at the same time, reduces the unburnt brick material's water absorption. The suitable weight content of Na_2SiO_3 solution and waste stone powder for the fabrication of unburnt bricks is 0.5 wt% and 23 wt%, respectively, in the total weight. With the formula, the obtained unburnt brick has a compressive strength of 10.9 ± 0.6 MPa, a water absorption of 8.8% and a water permeability of 12.4%. These parameters meet the standard of unburnt bricks of grade M10 according to TCVN 6477:2016 standard.

Acknowledgments

This work was supported by Polymer Centre, A&A Green Phoenix Group Joint Stock Company.

References

[1] J. Davidovits, Geopolymer Chemistry and Applications. 5-th edition, Institut Géopolymère, Saint-Quentin, France, 2020.

[2] W. W. A. Zailani, A. Bouaissi, M. M. Al Bakri Abdullah, R. Abd Razak, S. Yoriya, M. A. A. Mohd Salleh, M. A. Z. Mohd Remy Rozainy, H. Fansuri, Bonding strength characteristics of FA-based geopolymer paste as a repair material when applied on opc substrate, Appl. Sci. 10, 1-14, 2020, https://doi.org/10.3390/app10093321

[3] S. A. P. Rosyidi, S. Rahmad, N. I. M. Yusoff, A. H. Shahrir, A. N. H. Ibrahim, N. F. N. Ismail, K. H. Badri, Investigation of the chemical, strength, adhesion and morphological properties of fly ash based

geopolymer-modified bitumen, Constr. Build. Mater. 255, 119364, 2020. https://doi.org/10.1016/j.conbuildmat.2020.119364

[4] M. Xia, B. Nematollahi, J. Sanjayan, Printability, accuracy and strength of geopolymer made using powder-based 3D printing for construction applications, Autom. Constr. 101, 179-189, 2019. https://doi.org/10.1016/j.autcon.2019.01.013

[5] P. Nuaklong, V. Sata, P. Chindaprasirt, Properties of metakaolin-high calcium fly ash geopolymer concrete containing recycled aggregate from crushed concrete specimens, Constr. Build. Mater. 161, 365-373, 2018, https://doi.org/10.1016/j.conbuildmat.2017.11.152

[6] K. Lu, B. Wang, Z. Han, R. Ji, Experimental study of magnesium ammonium phosphate cements modified by fly ash and metakaolin, J. Build. Eng. 51, 2022, https://doi.org/10.1016/j.jobe.2022.104137

[7] E. Molaei Raisi, J. Vaseghi Amiri, M.R. Davoodi, Mechanical performance of self-compacting concrete incorporating rice husk ash, Constr. Build. Mater. 177, 148-157, 2018, https://doi.org/10.1016/j.jclepro.2019.119797.

[8] N. Q. Phu, N. T. Le, Study on using sea sand, combining fly ash and granulated blast furnace slag to manufacture the polymer concrete applications for irrigation works, Journal of Construction Sience and Technology 3th, 2021.

[9] E. Arioz, O. Arioz, O. M. Kockar, Geopolymer Synthesis with Low Sodium Hydroxide Concentration, Iran. J. Sci. Technol. - Trans. Civ. Eng. 44, 525-533, 2020, https://doi.org/10.1007/s40996-019-00336-1.

[10] C. A. Rees, J. L. Provis, G. C. Lukey, J. S. J. Van Deventer, In Situ ATR-FTIR Study of the Early Stages of Fly Ash Geopolymer Gel Formation, Langmiur, 23, 9076-9082, 2007, https://doi.org/10.1021/la701185g.

[11] Z. Wang, Y. Sun, S. Zhang, Y. Wang, Effect of sodium silicate on Portland cement/calcium aluminate cement/gypsum rich-water system: Strength and microstructure, RSC Adv. 9, 9993-10003, 2019, https://doi.org/10.1039/c8ra09901d.

[12] I. Hager, Colour Change in Heated Concrete, Fire Technol. 50, 945-958, 2014. https://doi.org/10.1007/s10694-012-0320-7.